Sfrp1 deficiency makes retinal photoreceptors prone to degeneration

Fabiana di Marco[1*], Elsa Cisneros[1,2*+], Javier Rueda-Carrasco[1], Concepción Lillo[3], María Jesús Martín-Bermejo[1], África Sandonís[1,2], Pilar Esteve[1,2] and Paola Bovolenta[1,2#]

[1]*Centro de Biología Molecular Severo Ochoa, CSIC-UAM and* [2]*Centro de Investigación Biomédica en Red de Enfermedades Raras (CIBERER). Madrid, Spain.* [3]*Departamento de Biología Celular y Patología. Universidad de Salamanca, Instituto de Neurociencias de Castilla y León and IBSAL. Salamanca, Spain*

*Equally contributing authors

+Present address: Centro Universitario Internacional de Madrid (CUNIMAD), Dept. de Biología de Sistemas, Universidad de Alcalá. Madrid, Spain

Corresponding author at: Centro de Biología Molecular Severo Ochoa, UAM/CSIC. c/ Nicolás Cabrera 1. Campus de la Universidad Autónoma de Madrid. 28049 Madrid, Spain. Phone: (+34) 911964718. Fax: (+34) 911964420. e-mail: pbovolenta@cbm.csic.es

authors' e-mail address

Fabiana di Marco, dm.fabiana@hotmail.it

Elsa Cisneros, elsa.cisneros@gmail.com

Javier Rueda-Carrasco, jrueda@cbm.csic.es

Concepción Lillo, conlillo@usal.es

María Jesús Martín-Bermejo, cbermejo@cbm.csic.es

África Sandonís, sandonisa@yahoo.es

Pilar Esteve, pesteve@cbm.csic.es

Paola Bovolenta, pbovolenta@cbm.csic.es

Abstract

Background: Genetic and age-related photoreceptor degeneration impairs vision in millions of individuals worldwide, often enhanced by factors that modify the genotype-phenotype correlation, independently of the primary cause of the disease. Secreted Frizzled Related Protein 1 (SFRP1), a modulator of Wnt signalling and of the enzymatic activity of the α-sheddase ADAM10, seems to be upregulated in human retinas affected by retinitis pigmentosa, a genetic disease leading to photoreceptors' degeneration. Here we have asked whether SFRP1 contributes to photoreceptor degeneration.

Methods: Adult mice deficient in the *Sfrp1* gene were used to address the implication of SFRP1 in maintaining retinal homeostasis in normal and photo-damaged conditions. Molecular and morphological preservation of the retinas was evaluated by western blot as well as histological, *in situ* hybridisation and immunohistochemical analysis using confocal and transmission electron microscopy. Visual function was assessed by electroretinography.

Results: In *Sfrp1* null mice, the outer limiting membrane (OLM) was discontinuous and the photoreceptors were disorganized and more prone to light-induced damage, significantly enhancing the effect of the $Rpe65^{Leu450Leu}$ genetic variant -present in the mouse genetic background- which confers sensitivity to light-induced stress. These alterations worsened with age and led to a significant decrease in visual function. These defects were associated to an increased proteolysis of Protocadherin 21 (PCDH21), an adhesion molecule localized to the inner portion of the photoreceptor outer segment, and N-cadherin, a component of the OLM.

Conclusions: SFRP1 contributes to photoreceptor fitness with a mechanism that involves the maintenance of OLM integrity. These conclusions are discussed in light of the initial observation that SFRP1 expression is upregulated in cases of retinitis pigmentosa and of the evidence that elevated levels of SFRP1 contribute to Alzheimer´s disease pathogenesis.

Keywords: Retina, Outer Limiting Membrane, Cell adhesion, photoreceptor degeneration, Retinitis Pigmentosa, Light-induced damage, Alzheimer's disease

Background

Photoreceptors are specialized neurons localized in the outermost layer of the retina, which are responsible for converting light information into electrical activity. There are two types of photoreceptors: cones that mediate vision in bright light (photopic vision), and rods that support vision in dim light (scotopic vision). Each photoreceptor develops a highly modified cilium, the outer segment (OS), composed of a stack of membranes that contains light-sensing visual pigments and other photo-transduction proteins connected to the photoreceptor cell body by the inner segment (IS). The organization, polarity and function of these specialized structures is assured at the proximal side by the presence of the outer limiting membrane (OLM), composed of a series of adherens junctions between the initial portion of the IS and the neighbouring Müller glial end-feet. At the distal side, instead, the OSs are in contact with the retinal pigment epithelium (RPE), a monolayer of cells that daily phagocyte the OS abutting portion and provides metabolic support to the photoreceptors (1). Thus, the physiology of photoreceptors is critically dependent, among others, on their interaction with adjacent non-neuronal cell types. Environmental, age-related and genetic defects disrupting these interactions lead to the progressive death of photoreceptors and thereby to the progressive loss of sight, often followed by total blindness (2). The most prevalent forms of this type of degeneration are Age-related Macular Degeneration (AMD) and specific forms of Retinitis Pigmentosa (RP) (2).

AMD has a complex aetiology that includes only partially understood environmental and genetic influences. The disease is characterized by impaired phagocytosis of the photoreceptors' OS by the RPE and inflammatory reactions that ultimately cause photoreceptor loss in the macula, a cone-enriched region of the human retina responsible for visual acuity (3). RP is instead a collection of monogenic disorders characterized by a tremendous genetic heterogeneity (4), involving genes expressed in the OS and OLM, such as PCDH21 (5) or Crumbs homolog 1 (CRB1) (6). The complexity of AMD and the heterogeneity of RP is further increased by the existence of incomplete penetrance and variability in the age of disease onset even among relatives carrying identical mutations or risk alleles (7). This indicates the importance of factors that, independently of the primary causes of the disease, contribute to modify the genotype-phenotype correlation. The identification of such factors may thus be instrumental in designing strategies for slowing down the progression of photoreceptors' degeneration. Although the nature of such factors is still largely elusive, neuroinflammatory conditions have been reported to enhance

photoreceptor degeneration (8, 9), as it happens in many different neurodegenerative diseases, including Parkinson's or Alzheimer's diseases (10).

In this context, we have recently shown that elevated levels of Secreted Frizzled-Related Protein (SFRP) 1- a secreted protein with the dual function of modulating Wnt signalling (11) and regulating the enzymatic activity of the α-sheddase ADAM10 (12)- contributes to the pathogenesis of Alzheimer's Disease (13). Consistent with the notion that ADAM10 cleaves a large number of substrates -including the amyloid precursor protein (APP) and proteins involved in the activation of microglial cells and in synaptic plasticity (14)-, high levels of SFRP1 prevent ADAM10-mediated non-amyloidogenic processing of APP (13) and favour neuroinflammation (15). *Sfrp1* and its homologues *Sfrp2* and *Sfrp5* have been implicated in different aspects of eye and retinal development (16-22). Furthermore, and in contrast to what observed in the adult mammalian brain, in which expression is minimal in homeostatic conditions (13, 23), SFRP1 and SFRP5 have been found expressed in the adult retina, mostly localized to the photoreceptor layer (24). *SFRPs* genes are an unlikely primary cause of RP in humans (25); however, their expression is notably increased and ectopically distributed in the retinas of individuals affected by RP (24, 26). These observations, together with the notion that *Sfrps* expression is upregulated in a variety of inflammatory conditions (27), raised the possibility that these molecules could modify the course of photoreceptor degeneration. Addressing this per se interesting question has the additional incentive of exploring whether there are commonalities between RP and Alzheimer's disease, two neurodegenerative diseases otherwise unrelated.

Perhaps contrary to expectations, we report here that SFRP1 exerts a protective role on retinal photoreceptors. In its absence, photoreceptors of young and mature mice showed subtle morphological alterations of the OS associated with discontinuities of the OLM and an increased proteolytical processing of two of its components: N-cadherin and PCDH21. Furthermore, the absence of *Sfrp1* significantly increased the sensitivity of the photoreceptors to light-induced damage in the presence of the sensitizing $Rpe65^{Leu450Leu}$ gene variant, present in the genetic background of the mice.

Methods

Animals. *Sfrp1*^{tm1Aksh} mice (*Sfrp1*$^{-/-}$ mice, thereafter), generated as described (28), were kindly provided by Dr. A. Shimono (TransGenic Inc. Chuo, Kobe, Japan) and maintained in a mixed C57BL/6 x 129 genetic background (B6;129). Mutant mice were compared with wild type (wt) littermates. All animals were housed and bred at the CBMSO animal facility in a 12 h light/dark cycle and treated according to European Communities Council Directive of 24 November 1986 (86/609/EEC) regulating animal research. All procedures were approved by the Bioethics Subcommittee of Consejo Superior de Investigaciones Científicas (CSIC, Madrid, Spain) and the Comunidad de Madrid under the following protocol approval number (PROEX 100/15; RD 53/2013).

Genotyping for Rpe65 and Crb1 variants. To determine which are the *Crb1* and *Rpe65* gene variants present in the genome of the mouse line used in this study, tail genomic DNA was isolated from *Sfrp1*$^{-/-}$ mice and their wt littermates according to standard protocols and genotyped as described (29, 30). To determine the sequence of *Crb1* and *Rpe65* we used the following primer pairs: *Crb1* Fw, 5'-GGTGACCAATCTGTTGACAATCC-3'; Rv, 5'-GCCCCATTTG CACACTGATGAC-3' (29); *Rpe65*; Fw, 5′-CTGACAAGCTCTGTAAG-3′; Rv, 5′-CATTACCATCAT CTTCTTCCA-3′ (29, 30). Amplified fragments were sequenced (Secugen S.L., Madrid) and analysed using CLC Sequence Viewer 6 (Qiagen).

In situ hybridization (ISH) and immunohistochemistry (IH). Mice were anesthetized with sodium pentobarbital and perfused intracardially with 4% PFA in 0.1 M phosphate buffer (PB). Alternatively, animals were euthanized by CO_2 inhalation and eyes were enucleated and fixed by immersion in 4% PFA in PB for 2 h. The anterior segment of the eye was removed and the eyecups were cryoprotected by equilibration in 15-30% sucrose gradation in PB, embedded in 7.5% gelatine/15% sucrose solution, frozen and sectioned at 16 µm. Sections were processed for in situ hybridization (ISH) as described (21) using a DIG-labelled anti-sense riboprobe for *Sfrp1*. When processed for immunohistochemistry (IH), the sections were incubated for 2 h at room temperature (RT) in a solution containing 1% BSA, 0.1% gelatine and 0.1% Triton X-100 in phosphate buffer saline (PBS). The sections were then incubated with primary antibodies diluted in blocking solution at 4°C overnight. Primary antibodies were the following: mouse anti-Rhodopsin K16-155C (31) (kindly provided by Dr. P. Hargrave, 1:100), rabbit anti-Guanine Nucleotide Binding protein (G protein Beta 3 subunit, GNB3; Abcam; 1:1000), rabbit anti-β-catenin (Abcam, 1:1000 mouse anti-N-cadherin (Invitrogen; 1:500), mouse anti-Glutamine Synthetase (GS; Millipore, 1:1000). Sections were

washed and incubated with the appropriate Alexa-Fluor 488 or 594-conjugated secondary antibodies (Molecular Probes, 1:1000) at RT for 90 min. After washing, the tissue was counterstained with Hoechst (Sigma), mounted in Mowiol and analysed with light (Leica DM500) or confocal microscopy (Zeiss LSM 710). Confocal images were acquired with identical settings. Figures display representative images. Every staining was performed in a minimum of 3 control and 3 mutant mice, obtaining equivalent results. Retina thickness was measured using Hoechst stained cryostat sections at 400 to 1800 µm from the optic nerve head at intervals of 200 µm. Mean ± SEM thickness calculated and plotted using Excel software. Student's t-test was applied for comparison between wt and mutant animals

Transmission electron microscopy. Eyes were fixed by immersion in 2% glutaraldehyde and 2% PFA in 0.1 M cacodylate buffer. Samples were treated with 1% osmium tetroxide, dehydrated and embedded in Epon 812. Semi-thin sections (0.7 µm) were stained with toluidine blue and observed by light microscopy (Leica DM500), whereas ultrathin sections were analysed by electron microscopy (Zeiss EM900). Distributions of cone nuclei were measured in central retina semi-thin sections of 3 wt or mutant mice at (2 or 6 months old) and statistics was calculated and plotted using Excel software. Student's t-test was applied for comparison between wt and mutant animals. At least 3 wt or mutant mice were analysed using electron microscopy. Figures display representative images.

Western blot analysis. Isolated retinal tissue including the RPE was incubated in 2 mM $CaCl_2$ at room temperature for 30 min and then in buffer containing 150 mM NaCl, 50 mM Tris pH 7.5, 1 mM EDTA, 1% NP-40, complete protease inhibitor cocktail and PMSF (Roche), as previously described (32). Total proteins (50 µg) were separated by SDS-PAGE and transferred onto PVDF membrane. Membranes were immersed in a solution of 5% non-fat milk and 0.1% Tween 20 in Tris Buffered Saline (TBS) for 2 h and then incubated with the appropriate primary antibodies diluted in blocking solution at 4ºC overnight. The primary antibodies used were: rabbit antiserum against the C-terminal domain of PCDH21 (a kind gift of Dr. A. Rattner; 1:10.000), mouse monoclonal antibody generated against the C-terminal domain of N-cadherin (Invitrogen; 1:500); anti-CRB1 (a kind gift of Dr. J. Wijnholds, 1:500), and mouse anti-α-tubulin (Sigma, 1:10.000), used as a loading control. The membranes were washed and incubated with horseradish peroxidase-conjugated rabbit or mouse antibodies followed by ECL Advanced Western Blotting Detection Kit (Amersham). The immune-reactive bands were quantified by densitometry and the amount of proteolyzed fragment was

estimated as the ratio of C-terminal fragment (CTF)/full length (FL)/α-tubulin band values. Western blots were repeated at least 3 times obtaining similar results.

Light-induced retinal damage. The pupils from 4 and 9 months-old mice were dilated by topical administration of 1% tropicamide (Alcón cusí) 30 min before light exposure and by a second administration after the first 4 h of exposure. The light exposure device consisted of cages with reflective interiors, in which freely moving animals were exposed, at the same time of the day, to 15000 lux of cool white fluorescent light for 8 h. Control animals were sacrificed before light exposure, whereas experimental animals were sacrificed 7 days after completed light exposure.

Electroretinography (ERG). Mice were dark-adapted overnight. All procedures were performed under dim red light. Animals were anesthetized by intra-peritoneal injection of ketamine (95 mg/Kg) and xylazine (5 mg/Kg). The body temperature was maintained with an electric heating pad. The pupils were dilated by topical administration of 1% tropicamide as above. A drop of 2% methylcellulose was then placed between the cornea and the silver electrode to maintain conductivity. VisioSystem Veterinary set up (SIEM Bio-Médicale) was used to deliver flash stimuli, as well as to amplify, filter and analyse photoreceptor responses. Rod responses (Scotopic ERG) were determined using stimulation intensities ranging from -2.8 to -0.2 log Cd s/m^2. Cone responses (Photopic ERG) were registered after 10 min adaptation to a 3 Cd/m^2 background light using stimulation intensities ranging from -0.35 to 0.35 log Cd s/m^2 and after 10 min adaptation to a 30.3 Cd/m^2 background light using a stimulation intensity of 0.35 log Cd s/m^2. Cone responses were also tested by flicker ERG using a stimulation intensity of 0.5 log Cd s/m^2 at frequencies of 10, 20 and 30 Hz, after 10 min adaptation to a 30.3 Cd/m^2 background light. ERGs were recorded in 4 months old mice, 5 wt and 6 mutant mice homozygotes for the protective *Rpe65*^{Leu450Met} gene variant, in 5 wt and 5 mutant mice heterozygotes for the protective *Rpe65*^{Leu450Met} gene variant and in 2 wt and 3 mutant mice without protective gene variant. ERGs were also recorded in 9 months old mice, 5 wt and 5 mutant mice homozygotes for the protective *Rpe65*^{Leu450Met} gene variant. Mean ± SEM values were calculated and plotted using Excel software. Student's t-test was applied for comparison between wt and mutant mice. ANOVA with posthoc Tukey was applied for comparison between control and light-damaged wt and mutant mice.

Results

Young adult Sfrp1$^{-/-}$ retinas show subtle defects in cone photoreceptor organization

The final goal of our study was to determine if increased expression of SFRP1 favours photoreceptor degeneration. We reasoned that, if this was the case, mice lacking Sfrp1 activity (*Sfrp1$^{-/-}$)* should be more resistant than their wild type (wt) counterparts to light-induced damage, taken as a frequently used experimental paradigm to study photoreceptor degeneration (33). *Sfrp1* does not seem to be required for mouse retinal development (17, 28, 34). However, there are somewhat controversial reports on its adult retinal localization (35, 36) and, to our knowledge, no specific information on its possible function in adult retinal homeostasis. We addressed these issues first.

To clarify *Sfrp1* distribution, we hybridized sections of 1 month-old mouse eyes with a specific probe. Our results supported the report by Liu et al. (35). High levels of *Sfrp1* were localized to the inner nuclear (INL) and the ganglion cell (GCL) layers. Lower levels were also found in the outer nuclear (or photoreceptor) layer (ONL; Fig. 1A), with a more abundant distribution in a subset of cells located at the outermost region (Fig. 1B, white arrows), in which the cell bodies of cone photoreceptors are found (37). Immunostaining with specific antibodies confirmed a similar layered distribution of the protein that, according to its secreted and dispersible nature (17, 38), was notably accumulated at the OLM/OS region (Fig. 1C,D).

To determine if the activity of Sfrp1 is required for the organization of the adult retina, we compared retinal morphology of 2 months-old *Sfrp1$^{-/-}$* and wt mice using toluidine blue stained semi-thin sections. No appreciable gross differences were detected between the two genotypes and the thickness of the ONL layer was comparable in both the dorsal and ventral quadrants (Fig. 1E,F,K; n=3 mice/ genotype). In mice, cone cell bodies are mostly arranged in a single row below the OLM with nuclei characterized by the presence of 1-3 irregular clumps of heterochromatin. Rods instead occupy all the ONL rows with more densely stained nuclei and a single large central clump of heterochromatin (37). This arrangement was easily recognizable in wt retinas observed at higher magnification (Fig. 1G), with 86.1% (± 0.2) of the cones localized to the first or second row of the ONL, whereas the remaining 13.9% (± 2.9) were found in other rows (n=3 mice). In *Sfrp1$^{-/-}$* retinas instead, cone nuclei were abnormally distributed (Fig. 1H, red asterisks) and only 51.1% (± 6.2) of the cone cell bodies were found in the first two rows. The remaining 48.9% (±3.1) were distributed in other rows, with a significant cone increase in deeper rows (n=3 mice; t-test $p<0.01$). Nonetheless, the

total number of cones was not significantly different between wt (291 ± 8, in nerve head sections, n=3) and *Sfrp1*$^{-/-}$ mice (336 ± 13.5, n=3; t-test), at least in young adults, although ultra-structural analysis revealed occasional degenerative signs in the OS of the mutants, which were never observed in wt (Fig. 1I,J).

Sfrp1$^{-/-}$ mice were bred in a mixed C57BL/6 x 129 background. Previous studies have warned that C57BL/6N sub-strain carries a single nucleotide deletion in the Crumb homologs 1 (*Crb1)* gene, which causes a retinal phenotype that may override that of other genes of interest (29). Our animals were bread in the C57BL/6J sub-strain, reported to carry a wt allele (29). Nevertheless, and to confirm that the observed defects were bona fide associated to the loss of *Sfrp1* function, we sequenced the *Crb1* gene in the *Sfrp1*$^{-/-}$ line. No *Crb1* mutations were found in all the analysed samples of our colony (not shown).

Once excluded the possible contribution of a defective *Crb1* allele, we next asked if the subtle defects observed in *Sfrp1*$^{-/-}$ retinas had an impact on photo-transduction or synaptic transmission between photoreceptors and bipolar cells. To this end, we compared the electrical responses of groups of 4-months old wt and *Sfrp1*$^{-/-}$ mice (n=12 per genotype) to light stimuli of increasing intensity and under increasing frequency. ERGs were recorded under scotopic (Fig. 2A,B) and photopic (Fig. 2C-E) conditions to evaluate rod/rod bipolar cells and cone/cone bipolar function, respectively. Mutant mice showed a small but significant decrease of photoreceptor (a-wave) scotopic responses at higher intensities (Fig. 2A,B) and a tendency towards a lower response under flicker stimuli of low frequency (Fig. 2C-E).

Together these data suggest that SFRP1 contributes to maintain retinal organization but its absence has negligible effects on young adults.

Retinal disorganization and visual performance of Sfrp1$^{-/-}$ *retinas worsen with age*

Photoreceptors disorganization, decreased OS length and scotopic responses together with reduced synaptic density and loss of melanin granules are among the alterations found in the aging mammalian retinas (39-41). The retinal phenotype of the young adult *Sfrp1*$^{-/-}$ mice shared some of these features, suggesting that the observed features could worsen with time.

To address this possibility gross retinal morphology of 6 months-old wt and *Sfrp1*$^{-/-}$ mice was analysed, finding no considerable macroscopic differences. However, the well-aligned columnar organization of the photoreceptors observed in wt was lost in the *Sfrp1*$^{-/-}$ retinas and, cone photoreceptor nuclei were distributed throughout the width of the ONL (Fig. 3A,B), as we observed in young mice. Many photoreceptors' nuclei were also misplaced past

the OLM that normally overlays the ONL (n=6, Fig. 3C,D). Retinal immunostaining with the Trasducin/GNB3 and rhodopsin (Rho), markers of the OS of cones and rods, respectively, confirmed subtle photoreceptors' alterations. Trasducin/GNB3 staining appeared reduced and fragmented in the mutant retinas (n=3 mice for each age, Fig. 3E,F), reflecting a small but significant reduction of the number cone nuclei counted in toluidine blue stained sections (wt, 231.6 ± 12 vs. *Sfrp1*$^{-/-}$ 183 ± 12.9, in retinal nerve head sections; n=3 mice, t-test, $p<0.05$). In wt mice, Rho normally localises to the OS (Fig. 3G), but in the *Sfrp1*$^{-/-}$ retinas labelling was also observed in the cell bodies of a number of cells (Fig. 3H). Although ONL cell density was an obstacle for precise evaluation of the proportion of affected rods, cells with abnormal Rho distribution were consistently observed in both eyes of all the analysed animals (n=3 mice for each age analysed, i.e., 6 and 8 month). These defects further worsened with ageing, so that in 12 months-old mutant animals the thickness of ONL was significantly reduced (20% on average) across the almost entire dorso-ventral axis of the retinas as compared to age matched wt (Fig. 3I; n=5 per genotype, t-test).

The presence of Rho in the cell bodies reflects cell intrinsic or OLM disturbances (42). Indeed, the OLM seals off the photoreceptor inner and outer segments from the rest of the cell, thereby limiting the diffusion of the photo-transduction cascade components (43). This notion together with the displacement of the photoreceptor nuclei (Fig. 3C, D), similar to that observed upon pharmacological disruption of the OLM (44, 45), suggested the existence of OLM alterations in the mutants. The intermittent brakeage of the OLM already apparent in histological sections (red arrows in Fig. 3D) was confirmed by transmission electron microscopic analysis (n=3). The well-organized arrangement of zonula adherens junctional complexes between the plasma membranes of the photoreceptor ISs and the apical processes of Müller glia that compose the OLM was readily visible in wt retinas (Fig. 4A). This arrangement was no longer present in those regions of the *Sfrp1*$^{-/-}$ retinas in which photoreceptors' nuclei were displaced bearing occasional signs of degeneration (Fig. 4B). Mutant retinas showed also less and smaller melanosomes in RPE cells (Fig 4C,D) and alterations in the synaptic contacts between photoreceptors and bipolar interneurons, such as an abnormal accumulation of synaptic vesicles (Fig. 4F), the degeneration of pre and post-synaptic terminals (red arrows in Fig. 4G,H) and mitochondrial disorganization (yellow arrow in Fig. 4G). None of these defects were observed in wt retinas (Fig. 4E) but have been reported in aging retinas (39-41).

Recording of ERGs responses under scotopic (Fig. 4I, J) and photopic (Fig. 4K-N) conditions in 9 months-old wt and *Sfrp1*$^{-/-}$ mice showed that the above described

morphological defects of *Sfrp1*$^{-/-}$ mice were associated with a poorer performance of both rod and rod bipolar cells (Fig. 4I, J) and cone and cone bipolar cells (Fig. 4K,L), as compared to wt mice (n=5 per genotype). Direct comparison of the photopic responses of 4 and 9 months-old *Sfrp1*$^{-/-}$ mice clearly shown a progressive deterioration with aging (Fig. 4M, N).

Together these data indicate that *Sfrp1* loss causes a slow but progressive deterioration of the retinal integrity associated with a gradual decrease of visual function.

The proteolysis of OLM and OS components is increased in Sfrp1$^{-/-}$ *retinas*

The region of the OLM is enriched in cell adhesion molecules, such as N-cadherin found at the adherens junctions (46) and protocadherin PCDH21, located at the base of the OS (47). Other transmembrane molecules are, for example, CRB2 and CRB1, found at the subapical region (right above the adherens junctions) of the photoreceptors and/or Müller glial cells as part of a large protein complex (6). As already mentioned, a tight adhesion between IS of the photoreceptors and the end feet of the Müller cells is critical for photoreceptor integrity and retinal organization (48). Furthermore, variation of the human CRB1 and CRB2 genes are responsible of retinal dystrophies such as RP (49) and inactivation of their murine homologues disrupts the OLM and causes photoreceptor loss (50). We thus reasoned that the retinal phenotype of the adult *Sfrp1*$^{-/-}$ mice could be mechanistically linked to poor Müller/photoreceptor cell adhesion, which, in turn, would be responsible of photoreceptor alterations. This mechanism is based on the notion that SFRP1 acts as a negative modulator of ADAM10 (12, 13, 21, 23), which proteolytically removes the ectodomains (ectodomain shedding) of a large number membrane proteins (51), including cell adhesion molecules such as Cadherins and proto-Cadherins (52-54), thereby controlling cell-cell interactions (51, 54). Different ADAM proteins, including ADAM10, have been found expressed in different retinal layers and cell types, comprising photoreceptors and Müller cells (55). Furthermore, abnormal proteolytical processing of OS components influences photoreceptor degeneration (32) and SFRP1 is particularly abundant in the OLM/OS region (Fig. 1C,D), suggesting that in its absence ADAM10-mediated proteolysis could be more efficient.

We therefore tested if an enhanced proteolytical processing of N-cadherin and/or PCDH21 could explain the retinal alterations of *Sfrp1*$^{-/-}$ mice. To this end, we compared by Western blot analysis the proportion of proteolyzed versus full-length protein levels of N-cadherin and PCDH21 in wt, *Sfrp1*$^{-/-}$ and *rd10* mice. These mice, carrying a missense mutation in the rod specific *Pde6b*, are a widely used model of fast photoreceptor degeneration (56) and thus appeared useful to assess mechanistic specificity. Proteolytical

processing of full-length N-cadherin (135 kD) results in the generation of a C-terminal intracellular peptide of 35 kDa (54), whereas the 120 kDa full length PCDH21 is cleaved in two fragments of 95 (N-terminal) and 25 (C-terminal) kDa (32). Antibodies against the C-terminal portion of either N-Cadherin or PCDH21 were probed against retinal extracts of three weeks-old mice. At this stage, the majority of photoreceptors in *rd10* mice are still alive, allowing for comparison. *Sfrp1*$^{-/-}$ retinal extracts contained an increased proportion of the C-terminal fragments of both N-cadherin and PCDH21 when compared to those detected in wt (Fig. 5A,B; about 2- and 3.5-fold, respectively). N-cadherin but not PCDH21 proteolysis was also observed in *rd10* retinas (Fig. 5A,B). Comparable levels of CRB1 were present in the three genotypes (Fig. 5C), supporting similarities in photoreceptors' content at this stage. Furthermore, the signal of immunostaining for N-cadherin and β-catenin -which functionally interacts with cadherins at the adherens junctions (57)- appeared discontinuous and spread along the Müller glial processes in the *Sfrp1*$^{-/-}$ retinas (Fig. 5E,G) but a continuous line in wt retinas (Fig. 5D,F). Staining of Müller glial cells with anti-Glutamine Synthetase (GS) confirmed the discontinuous arrangement of their apical end-feet in the mutants but not in the wt retina (Fig. 5H,I).

Altogether these data indicate that Sfrp1 indirectly regulates photoreceptors/Müller glia interaction, which is, in turn, essential for retinal integrity and optimal function.

Sfrp1 bestow resistance to the photoreceptors upon light induced damage

If Sfrp1 maintains photoreceptor integrity, in its absence photoreceptors should be more sensitive to a neurodegenerative stimulus. Exposure to high intensity light is an experimental paradigm widely used to induce a rhodopsin mediated stereotypic photoreceptor apoptosis (33), to which cones are less susceptible (58, 59). The degree of response however varies according to the pigmentation and genetic background of the animals (33). Most prominently, a Leu450Met variation in the retinal pigment epithelium *Rpe65* gene, found in the C57BL/6 and 129 mouse strains (30), confers resistance to light damage. Given the genetic background of the *Sfrp1*$^{-/-}$ mice, we sequenced the *Rpe65* gene in our colony, finding the presence the *Rpe65*^{Leu450Met} variant mostly in heterozygosis. To clearly separate the contribution of the two alleles we generated *Rpe65*^{Leu450Leu}*;Sfrp1*$^{-/-}$ and *Rpe65e*^{Leu450Met}*;Sfrp1*$^{-/-}$ animals and their respective controls.

We thereafter exposed 4 months-old wt and *Sfrp1*$^{-/-}$ mice carrying the two *Rpe65* variants to a 15.000 lux light source for 8 h and analysed the extend of photoreceptors' loss by immunohistochemical analysis seven days after treatment. Under these conditions and

compared to untreated animals (the two *Rpe65* variant were undistinguishable), the retinas of *Rpe65e*^{Leu450Met}*;Sfrp*$^{+/+}$ mice were only slightly affected. The morphology and thickness of their ONL as well as the immunolabelling for rod (Rho) and cones (GNB3) markers were comparable to that of untreated animals (Fig. 6A,C,E,G,M). Given the absence of the resistence allele, the photoreceptors of *Rpe65e*^{Leu450Leu}*;Sfrp*$^{+/+}$ mice instead presented signs of disorganization and the ONL was slightly thinner in central regions as compared to untreated mice (Fig. 6A,C,I,K,N). By contrast, the retinas of *Rpe65e*^{Leu450Met}*;Sfrp1*$^{-/-}$ and, to a larger extend, those of *Rpe65*^{Leu450Leu}*;Sfrp1*$^{-/-}$ mice were visibly affected by light damage. There was a central^{high} to peripheral^{low} loss of both rod and cones photoreceptors with abnormal localisation of Rho in rod cell bodies (Fig. 6B,D,F,H,J,L,N). As compared to rod, cone loss appeared proportionally more significant in the presence of the *Rpe65*^{Leu450Leu} than in the *Rpe65e*^{Leu450Met} variant (compare Fig. 6F,H with J,L).

Comparative recording of ERGs responses from *Rpe65e*^{Leu450Leu}*;Sfrp*$^{+/+}$ and *Rpe65e*^{Leu450Leu}*;Sfrp1*$^{-/-}$ 4 months-old mice exposed or not to light damage extended this analysis. Untreated mice lacking *Sfrp1* presented a slightly reduced rod (scotopic) and cone (photopic) response to light flashes compared to *Sfrp1*$^{+/+}$ (Fig. 7A-D). Consistently the reduced loss of photoreceptors observed in *Rpe65e*^{Leu450Leu}*;Sfrp*$^{+/+}$ after damage (Fig. 6E,C), both scotopic and photopic responses were only slightly and non-significantly reduced in these animals (Fig. 7A-D). High intensity light exposure instead strongly reduced the rod and cone response of *Rpe65e*^{Leu450leu}*;Sfrp1*$^{-/-}$ mice (Fig. 7A-D) with an additional important decrease of the response under flicker stimuli of low frequency (Fig. 7E).

All in all, these data indicate that Sfrp1 activity critically supports photoreceptor integrity and function upon a neurodegenerative stimulus.

Discussion

The progression of photoreceptor neurodegeneration is variable among individuals affected by RD, even when caused by identical hereditary mutations. The reasons of this variability are largely unknown but the identification of relevant factors may help explain these differences and perhaps define strategies to restrain vision loss. This approach may be particularly important when applied to cones because these neurons are activated by day-light or artificial illumination and their degeneration is often an aftermath of rod or RPE alterations. Thus, sparing cone cell death would be sufficient to preserve the well-being of many patients (60). The reported increase of SFRP1 expression in cases of RP (24, 26) together with the observation that neutralization of SFRP1 significantly improves several Alzheimer's like features in a mouse model (13), made us test the possible implication of SFRP1 in photoreceptors' degeneration. Perhaps in contrast to our expectation, in this study, we show that Sfrp1 helps maintaining photoreceptors' fitness and protects them from light induced damage. Mechanistically, SFRP1 favours the tight cell adhesion responsible for the integrity of OLM, a structure important for photoreceptor survival and proper function.

Overexpression studies in the embryonic chick retina indicate that *Sfrp1* promotes cone generation (18). Nevertheless, *Sfrp1*$^{-/-}$ eyes show no developmental defects (17, 28, 34) likely because the retinal expression of the related *Sfrp2* and *Sfrp5* compensates its function during development (12, 17, 35, 61). In this study we have shown that sparse signs of cone alterations, such as an atypical position of their nuclei and OS de-compaction, can be detected in young adult *Sfrp1*$^{-/-}$ mice. These defects worsened with time when additional subtle rods' alterations appear together with a progressive impoverishment of visual function, signs that are characteristic of retinal ageing (62, 63).

SFRP proteins have been initially discovered and described as apoptosis-related proteins (64). We cannot fully discard that SFRP1 may in part act in the retina with such an activity. However, whereas Sfrp2 and Sfrp5 have anti-apoptotic functions (64, 65), Sfrp1 overexpression increases cell sensitivity to pro-apoptotic stimuli (64), making the defects observed in *Sfrp1*$^{-/-}$ retina hardly interpretable through an apoptosis related mechanism. Inhibition of Wnt signalling, a Sfrp1 function observed in many different contexts (11), is also unlikely in the adult retina, because photoreceptors are significantly less vulnerable to light-induced damage upon Wnt signalling activation (66), which is the opposite of what we observe in *Sfrp1*$^{-/-}$ mice. Instead, our data best explain the *Sfrp1*$^{-/-}$ retinal phenotype according to the following model (Fig. 8), based on Sfrp1-mediated inhibition of the metalloprotease

ADAM10 (12, 13). Sfrp1, produced by photoreceptors and possibly Müller glial cells, down-regulates ADAM10 activity at the OLM, thereby maintaining the required tight adhesion between the end-feet of Müller cells and the IS of the photoreceptors. In its absence, the increased proteolysis of the OLM and OS components loosen the OLM, progressively impairing photoreceptors' anchorage. The OLM confers mechanical strength to the retina and limits the diffusion of components of the photo-transduction cascade. Its loosening sets the conditions for a decreased photoreceptor fitness that makes cells more sensitive to light, and possibly, to other types of stress (Fig. 8). This model is supported by the appropriate localization of the required molecular machinery -ADAM10, SFRP1 and different cell adhesion molecules- within the retina (46, 47, 55, 67) and this study) and by the increased shedding of N-cadherin and PCDH21 in the *Sfrp1*$^{-/-}$ retinas. Increased proteolysis of these molecules has been shown to weaken cell-cell interactions (53, 54) and thus may well explain the intermittent breakage of the OLM in the *Sfrp1*$^{-/-}$ retinas, with the consequent disorganization of the ONL and rhodopsin distribution. The latter defect is considered both a consequence and a further cause of rod degenerative signs, including the decompaction of the OS disc membrane stacks (68), as we observed in the *Sfrp1*$^{-/-}$ mutants.

In further support of our findings, missense mutations in PCDH21 have been identified in patients affected by autosomal recessive cone-rod dystrophy (5, 69), suggesting that this protocadherin might be particularly relevant for cone survival. Indeed, its targeted disruption in mice causes OS fragmentation followed by a relatively mild decrease of the ERG response and photoreceptors' loss (32), somewhat resembling the *Sfrp1*$^{-/-}$ retinal phenotype. However, the precise relationship between PCDH21 shedding and photoreceptor degeneration might not be so straightforward. Analysis of PCDH21 shedding in mice that lack peripherin (*rds*$^{-/-}$), a structural OS protein, revealed higher levels of protein expression and a decreased proteolysis (32) and we show that in *rd10* mice PCDH21 proteolysis was similar to wt. The reasons for these differences likely reflect the primary genetic causes of photoreceptors degeneration in *rd10* and *rds* mice: PCDH21 and peripherin have structural functions whereas *rd10* mice carry a mutation in a component of the rod phototransduction cascade (56). Changes in cell adhesion might therefore be a consequence rather a main cause in *rd10* mice.

Besides highlighting a specific role of Sfrp1 in the adult retina, our study provides an additional physiological example in which Sfrp1 likely acts as an endogenous inhibitor of ADAM10, a conclusion that matches our previous findings (12, 13, 21, 23). In homeostatic conditions, Sfrp1 expression is barely detectable in the cortex of young and healthy

individuals but it expression increases with aging (70) and is upregulated in individual affected by Alzheimer's disease (13). In this condition, activated glial cells (particularly astrocytes) produce SFRP1 leading to increased levels of toxic products of amyloid precursor protein processing (13) and further sustaining chronic inflammation (15). In the adult retina, both neurons and likely Müller glial cells normally produce Sfrp1, which has a homeostatic function. However, photoreceptor degeneration is associated to neuroinflammation (8, 71, 72) and this should lead to a change in *Sfrp1* expression, explaining the reported upregulation and ectopic expression of SFRP1 in RP (24, 26). This abnormal SFRP1 production is likely to antagonize its protective and homeostasis role. Testing whether these two mechanisms counterbalance one another is not straightforward and deleterious effects are likely to prevail after damage. *SFRP1* expression is under strong epigenetic regulation (27) and this type of regulation could contribute to tune SFRP1 protective or offensive role in the retina.

Conclusions

In conclusion, we show that Sfrp1 contribute to adult retinal homeostasis maintaining the integrity of the OLM. The phenotype observed in *Sfrp1* null mice suggest the possibility that the age-related decrease of retinal fitness and visual performance might involve a progressive down-regulation of *Sfrp1* expression. Furthermore, differential *SFRP1* expression among individuals may represent one of the many possible causes of the low genotype-phenotype correlation observed among individuals suffering of retinal dystrophies.

List of abbreviations

AMD	Age-related Macular Degeneration
APP	amyloid precursor protein
CRB1	Crumbs homolog 1
CTF	C-terminal fragment
ERG	Electroretinogram
FL	Full length
GCL	Ganglion cell layer
GNB3	G protein Beta 3 subunit

GS	Glutamine Synthetase
IH	Immunohistochemistry
INL	Inner nuclear layer
IS	Inner segment
ISH	In situ hybridization
OLM	Outer limiting membrane
ONL	Outer nuclear layer
OS	Outer segment
PB	Phosphate buffer
PBS	Phosphate buffer saline
PCDH21	Protocadherin 21
PFA	Paraformaldehyde
Rho	Rhodopsin
RP	Retinitis Pigmentosa
RPE	Retinal pigment epithelium
RT	Room temperature
SEM	Standard error of the mean
SFRP	Secreted Frizzled Related Protein
TBS	Tris Buffered Saline
wt	Wildtype

Declarations

Ethics approval: Animals were housed and treated according to European Communities Council Directive of 24 November 1986 (86/609/EEC) regulating animal research. All procedures were approved by the Bioethics Subcommittee of Consejo Superior de Investigaciones Científicas (CSIC, Madrid, Spain) and the Comunidad de Madrid under the following protocol approval number (PROEX 100/15; RD 53/2013).

***Consent for publication*:** Not applicable

***Availability of data and materials*:** All data generated or analysed during this study are included in this published article

***Competing interests*:** The authors declare that they have no competing interests

***Funding*.** Supported by grants from Fundaluce, Fundación ONCE, Retina España and from the Spanish MINECO (BFU2010-16031; BFU2013-43213-P; BFU2016-75412-R with

FEDER support). A CBMSO Institutional grant from the Fundación Ramon Areces is also acknowledged. EC and AS were supported by the CIBERER and JRC was recipient of by FPI fellowships (BES-2011-047189). We also acknowledge support of the publication fee by the CSIC Open Access Publication Support Initiative through its Unit of Information Resources for Research (URICI).

Authors' contributions: EC and FM designed the experiments, performed and analysed experiments and contributed to manuscript preparation. JRC participated in immune-histochemical and ERG studies. CL performed and analysed EM studies. MJB and AS genotyped animals and performed biochemical analysis. PE participated in experimental design, result discussion and manuscript preparation. PB conceived the study, contributed to experimental design and interpretation and wrote the manuscript.

***Acknowledgements*:** The authors thank O. Herreras (Cajal Institute, CSIC) and E. Martín (Universidad de Albacete) for advice and support in the initial ERG studies.

References

1. Letelier J, Bovolenta P, Martinez-Morales JR. The pigmented epithelium, a bright partner against photoreceptor degeneration. J Neurogenet. 2017;31(4):203-15.
2. Wert KJ, Lin JH, Tsang SH. General pathophysiology in retinal degeneration. Dev Ophthalmol. 2014;53:33-43.
3. Mitchell P, Liew G, Gopinath B, Wong TY. Age-related macular degeneration. Lancet. 2018;392(10153):1147-59.
4. https://sph.uth.edu/Retnet/.
5. Ostergaard E, Batbayli M, Duno M, Vilhelmsen K, Rosenberg T. Mutations in PCDH21 cause autosomal recessive cone-rod dystrophy. J Med Genet. 2010;47(10):665-9.
6. Alves CH, Pellissier LP, Wijnholds J. The CRB1 and adherens junction complex proteins in retinal development and maintenance. Prog Retin Eye Res. 2014;40:35-52.
7. Pacione LR, Szego MJ, Ikeda S, Nishina PM, McInnes RR. Progress toward understanding the genetic and biochemical mechanisms of inherited photoreceptor degenerations. Annu Rev Neurosci. 2003;26:657-700.
8. Peng B, Xiao J, Wang K, So KF, Tipoe GL, Lin B. Suppression of microglial activation is neuroprotective in a mouse model of human retinitis pigmentosa. J Neurosci. 2014;34(24):8139-50.
9. Sene A, Apte RS. Inflammation-Induced Photoreceptor Cell Death. Adv Exp Med Biol. 2018;1074:203-8.
10. McKenzie JA, Spielman LJ, Pointer CB, Lowry JR, Bajwa E, Lee CW, et al. Neuroinflammation as a Common Mechanism Associated with the Modifiable Risk Factors for Alzheimer's and Parkinson's Diseases. Curr Aging Sci. 2017;10(3):158-76.
11. Bovolenta P, Esteve P, Ruiz JM, Cisneros E, Lopez-Rios J. Beyond Wnt inhibition: new functions of secreted Frizzled-related proteins in development and disease. Journal of cell science. 2008;121(Pt 6):737-46.

12. Esteve P, Sandonis A, Cardozo M, Malapeira J, Ibanez C, Crespo I, et al. SFRPs act as negative modulators of ADAM10 to regulate retinal neurogenesis. Nat Neurosci. 2011;14(5):562-9.
13. Esteve P, Rueda-Carrasco J, Ines Mateo M, Martin-Bermejo MJ, Draffin J, Pereyra G, et al. Elevated levels of Secreted-Frizzled-Related-Protein 1 contribute to Alzheimer's disease pathogenesis. Nat Neurosci. 2019;22(8):1258-68.
14. Saftig P, Lichtenthaler SF. The alpha secretase ADAM10: A metalloprotease with multiple functions in the brain. Prog Neurobiol. 2015;135:1-20.
15. Rueda J, et al.,. 2019.
16. Esteve P, Lopez-Rios J, Bovolenta P. SFRP1 is required for the proper establishment of the eye field in the medaka fish. Mechanisms of development. 2004;121(7-8):687-701.
17. Esteve P, Sandonis A, Ibanez C, Shimono A, Guerrero I, Bovolenta P. Secreted frizzled-related proteins are required for Wnt/beta-catenin signalling activation in the vertebrate optic cup. Development. 2011;138(19):4179-84.
18. Esteve P, Trousse F, Rodriguez J, Bovolenta P. SFRP1 modulates retina cell differentiation through a beta-catenin-independent mechanism. Journal of cell science. 2003;116(Pt 12):2471-81.
19. Holly VL, Widen SA, Famulski JK, Waskiewicz AJ. Sfrp1a and Sfrp5 function as positive regulators of Wnt and BMP signaling during early retinal development. Dev Biol. 2014;388(2):192-204.
20. Lopez-Rios J, Esteve P, Ruiz JM, Bovolenta P. The Netrin-related domain of Sfrp1 interacts with Wnt ligands and antagonizes their activity in the anterior neural plate. Neural development. 2008;3:19.
21. Marcos S, Nieto-Lopez F, Sandonis A, Cardozo MJ, Di Marco F, Esteve P, et al. Secreted frizzled related proteins modulate pathfinding and fasciculation of mouse retina ganglion cell axons by direct and indirect mechanisms. J Neurosci. 2015;35(11):4729-40.
22. Sugiyama Y, Shelley EJ, Wen L, Stump RJ, Shimono A, Lovicu FJ, et al. Sfrp1 and Sfrp2 are not involved in Wnt/beta-catenin signal silencing during lens induction but are required for maintenance of Wnt/beta-catenin signaling in lens epithelial cells. Dev Biol. 2013;384(2):181-93.
23. Esteve P, Crespo I, Kaimakis P, Sandonis A, Bovolenta P. Sfrp1 Modulates Cell-signaling Events Underlying Telencephalic Patterning, Growth and Differentiation. Cereb Cortex. 2019;29(3):1059-74.
24. Jones SE, Jomary C, Grist J, Stewart HJ, Neal MJ. Modulated expression of secreted frizzled-related proteins in human retinal degeneration. Neuroreport. 2000;11(18):3963-7.
25. Garcia-Hoyos M, Cantalapiedra D, Arroyo C, Esteve P, Rodriguez J, Riveiro R, et al. Evaluation of SFRP1 as a candidate for human retinal dystrophies. Mol Vis. 2004;10:426-31.
26. Jones SE, Jomary C, Grist J, Stewart HJ, Neal MJ. Altered expression of secreted frizzled-related protein-2 in retinitis pigmentosa retinas. Invest Ophthalmol Vis Sci. 2000;41(6):1297-301.
27. Esteve P, Bovolenta P. The advantages and disadvantages of sfrp1 and sfrp2 expression in pathological events. Tohoku J Exp Med. 2010;221(1):11-7.
28. Satoh W, Gotoh T, Tsunematsu Y, Aizawa S, Shimono A. Sfrp1 and Sfrp2 regulate anteroposterior axis elongation and somite segmentation during mouse embryogenesis. Development. 2006;133(6):989-99.
29. Mattapallil MJ, Wawrousek EF, Chan CC, Zhao H, Roychoudhury J, Ferguson TA, et al. The Rd8 mutation of the Crb1 gene is present in vendor lines of C57BL/6N mice and embryonic stem cells, and confounds ocular induced mutant phenotypes. Invest Ophthalmol Vis Sci. 2012;53(6):2921-7.
30. Wenzel A, Reme CE, Williams TP, Hafezi F, Grimm C. The Rpe65 Leu450Met variation increases retinal resistance against light-induced degeneration by slowing rhodopsin regeneration. J Neurosci. 2001;21(1):53-8.

31. Adamus G, Zam ZS, Arendt A, Palczewski K, McDowell JH, Hargrave PA. Anti-rhodopsin monoclonal antibodies of defined specificity: characterization and application. Vision Res. 1991;31(1):17-31.
32. Rattner A, Chen J, Nathans J. Proteolytic shedding of the extracellular domain of photoreceptor cadherin. Implications for outer segment assembly. J Biol Chem. 2004;279(40):42202-10.
33. Wenzel A, Grimm C, Samardzija M, Reme CE. Molecular mechanisms of light-induced photoreceptor apoptosis and neuroprotection for retinal degeneration. Prog Retin Eye Res. 2005;24(2):275-306.
34. Trevant B, Gaur T, Hussain S, Symons J, Komm BS, Bodine PV, et al. Expression of secreted frizzled related protein 1, a Wnt antagonist, in brain, kidney, and skeleton is dispensable for normal embryonic development. J Cell Physiol. 2008;217(1):113-26.
35. Liu H, Mohamed O, Dufort D, Wallace VA. Characterization of Wnt signaling components and activation of the Wnt canonical pathway in the murine retina. Dev Dyn. 2003;227(3):323-34.
36. Rattner A, Hsieh JC, Smallwood PM, Gilbert DJ, Copeland NG, Jenkins NA, et al. A family of secreted proteins contains homology to the cysteine-rich ligand-binding domain of frizzled receptors. Proc Natl Acad Sci U S A. 1997;94(7):2859-63.
37. Carter-Dawson LD, LaVail MM. Rods and cones in the mouse retina. I. Structural analysis using light and electron microscopy. J Comp Neurol. 1979;188(2):245-62.
38. Mii Y, Taira M. Secreted Frizzled-related proteins enhance the diffusion of Wnt ligands and expand their signalling range. Development. 2009;136(24):4083-8.
39. Bonilha VL. Age and disease-related structural changes in the retinal pigment epithelium. Clin Ophthalmol. 2008;2(2):413-24.
40. Kolesnikov AV, Fan J, Crouch RK, Kefalov VJ. Age-related deterioration of rod vision in mice. J Neurosci. 2010;30(33):11222-31.
41. Samuel MA, Zhang Y, Meister M, Sanes JR. Age-related alterations in neurons of the mouse retina. J Neurosci. 2011;31(44):16033-44.
42. Hollingsworth TJ, Gross AK. Defective trafficking of rhodopsin and its role in retinal degenerations. Int Rev Cell Mol Biol. 2012;293:1-44.
43. Omri S, Omri B, Savoldelli M, Jonet L, Thillaye-Goldenberg B, Thuret G, et al. The outer limiting membrane (OLM) revisited: clinical implications. Clin Ophthalmol. 2010;4:183-95.
44. Ishikawa Y, Mine S. Aminoadipic acid toxic effects on retinal glial cells. Jpn J Ophthalmol. 1983;27(1):107-18.
45. Rich KA, Figueroa SL, Zhan Y, Blanks JC. Effects of Muller cell disruption on mouse photoreceptor cell development. Exp Eye Res. 1995;61(2):235-48.
46. Matsunaga M, Hatta K, Takeichi M. Role of N-cadherin cell adhesion molecules in the histogenesis of neural retina. Neuron. 1988;1(4):289-95.
47. Rattner A, Smallwood PM, Williams J, Cooke C, Savchenko A, Lyubarsky A, et al. A photoreceptor-specific cadherin is essential for the structural integrity of the outer segment and for photoreceptor survival. Neuron. 2001;32(5):775-86.
48. West EL, Pearson RA, Tschernutter M, Sowden JC, MacLaren RE, Ali RR. Pharmacological disruption of the outer limiting membrane leads to increased retinal integration of transplanted photoreceptor precursors. Exp Eye Res. 2008;86(4):601-11.
49. Richard M, Roepman R, Aartsen WM, van Rossum AG, den Hollander AI, Knust E, et al. Towards understanding CRUMBS function in retinal dystrophies. Hum Mol Genet. 2006;15 Spec No 2:R235-43.
50. Quinn PM, Mulder AA, Henrique Alves C, Desrosiers M, de Vries SI, Klooster J, et al. Loss of CRB2 in Muller glial cells modifies a CRB1-associated retinitis pigmentosa phenotype into a Leber congenital amaurosis phenotype. Hum Mol Genet. 2019;28(1):105-23.
51. Lichtenthaler SF, Lemberg MK, Fluhrer R. Proteolytic ectodomain shedding of membrane proteins in mammals-hardware, concepts, and recent developments. EMBO J. 2018;37(15).

52. Kuhn PH, Colombo AV, Schusser B, Dreymueller D, Wetzel S, Schepers U, et al. Systematic substrate identification indicates a central role for the metalloprotease ADAM10 in axon targeting and synapse function. Elife. 2016;5.
53. Bouillot S, Tillet E, Carmona G, Prandini MH, Gauchez AS, Hoffmann P, et al. Protocadherin-12 cleavage is a regulated process mediated by ADAM10 protein: evidence of shedding up-regulation in pre-eclampsia. J Biol Chem. 2011;286(17):15195-204.
54. Reiss K, Maretzky T, Ludwig A, Tousseyn T, de Strooper B, Hartmann D, et al. ADAM10 cleavage of N-cadherin and regulation of cell-cell adhesion and beta-catenin nuclear signalling. Embo J. 2005;24(4):742-52.
55. Yan X, Lin J, Rolfs A, Luo J. Differential expression of the ADAMs in developing chicken retina. Dev Growth Differ. 2011;53(5):726-39.
56. Won J, Shi LY, Hicks W, Wang J, Hurd R, Naggert JK, et al. Mouse model resources for vision research. J Ophthalmol. 2011;2011:391384.
57. Harris TJ, Peifer M. Decisions, decisions: beta-catenin chooses between adhesion and transcription. Trends Cell Biol. 2005;15(5):234-7.
58. Okano K, Maeda A, Chen Y, Chauhan V, Tang J, Palczewska G, et al. Retinal cone and rod photoreceptor cells exhibit differential susceptibility to light-induced damage. J Neurochem. 2012;121(1):146-56.
59. Samardzija M, Todorova V, Gougoulakis L, Barben M, Notzli S, Klee K, et al. Light stress affects cones and horizontal cells via rhodopsin-mediated mechanisms. Exp Eye Res. 2019;186:107719.
60. Bovolenta P, Cisneros E. Retinitis pigmentosa: cone photoreceptors starving to death. Nat Neurosci. 2009;12(1):5-6.
61. Chang JT, Esumi N, Moore K, Li Y, Zhang S, Chew C, et al. Cloning and characterization of a secreted frizzled-related protein that is expressed by the retinal pigment epithelium. Hum Mol Genet. 1999;8(4):575-83.
62. Nadal-Nicolas FM, Vidal-Sanz M, Agudo-Barriuso M. The aging rat retina: from function to anatomy. Neurobiol Aging. 2018;61:146-68.
63. Salvi SM, Akhtar S, Currie Z. Ageing changes in the eye. Postgrad Med J. 2006;82(971):581-7.
64. Melkonyan HS, Chang WC, Shapiro JP, Mahadevappa M, Fitzpatrick PA, Kiefer MC, et al. SARPs: a family of secreted apoptosis-related proteins. Proc Natl Acad Sci U S A. 1997;94(25):13636-41.
65. Ruiz JM, Rodriguez J, Bovolenta P. Growth and differentiation of the retina and the optic tectum in the medaka fish requires olSfrp5. Dev Neurobiol. 2009;69(10):617-32.
66. Braunger BM, Ohlmann A, Koch M, Tanimoto N, Volz C, Yang Y, et al. Constitutive overexpression of Norrin activates Wnt/beta-catenin and endothelin-2 signaling to protect photoreceptors from light damage. Neurobiol Dis. 2013;50:1-12.
67. Toonen JA, Ronchetti A, Sidjanin DJ. A Disintegrin and Metalloproteinase10 (ADAM10) Regulates NOTCH Signaling during Early Retinal Development. PLoS One. 2016;11(5):e0156184.
68. Gao J, Cheon K, Nusinowitz S, Liu Q, Bei D, Atkins K, et al. Progressive photoreceptor degeneration, outer segment dysplasia, and rhodopsin mislocalization in mice with targeted disruption of the retinitis pigmentosa-1 (Rp1) gene. Proc Natl Acad Sci U S A. 2002;99(8):5698-703.
69. Henderson RH, Li Z, Abd El Aziz MM, Mackay DS, Eljinini MA, Zeidan M, et al. Biallelic mutation of protocadherin-21 (PCDH21) causes retinal degeneration in humans. Mol Vis. 2010;16:46-52.
70. Folke J, Pakkenberg B, Brudek T. Impaired Wnt Signaling in the Prefrontal Cortex of Alzheimer's Disease. Mol Neurobiol. 2019;56(2):873-91.

71. Ronning KE, Karlen SJ, Miller EB, Burns ME. Molecular profiling of resident and infiltrating mononuclear phagocytes during rapid adult retinal degeneration using single-cell RNA sequencing. Sci Rep. 2019;9(1):4858.
72. Rutar M, Natoli R, Chia RX, Valter K, Provis JM. Chemokine-mediated inflammation in the degenerating retina is coordinated by Muller cells, activated microglia, and retinal pigment epithelium. J Neuroinflammation. 2015;12:8.

Figures legends

Figure 1. SFRP1 is expressed in the retina and required for photoreceptor fitness. A-D) Frontal cryostat sections from 1 month-old wt animals hybridized (A, B), or immunostained (C,D) for Sfrp1 and counterstained with DAPI (D). The white arrows in B indicate the increased signal in the outermost region of the ONL. Note Sfrp1 accumulation in the OLM (arrowheads in C,D). **E-H)** Semi-thin sagittal sections from 2 months-old wt and *Sfrp1*$^{-/-}$ retinas stained with toluidine blue. Note the abnormal localization of the nuclei of cone photoreceptors in the mutant retina (red asterisks in H). **I, J)** TEM analysis of the OS. Note that in the mutants, but not in wt, the stacks of membranes of the OS are disorganized (red arrow in J). **K)** The graph shows the ONL thickness of 4 month-old wt and *Sfrp1*$^{-/-}$ retinas (measures were taken in cryostat frontal sections of the eye at the level of the optic disk). Abbreviations: GCL: ganglion cell layer; INL: inner nuclear layer; on: optic nerve; ONL: outer nuclear layer.

Figure 2. ***Sfrp1***$^{-/-}$ **retinas show slightly reduced visual function. A-D)** The graphs show the a- and b-wave amplitude (µV) of the scotopic (rods, A, B) and photopic (cones, C, D) ERG from 4 months-old WT and *Sfrp1*$^{-/-}$ animals to flash light stimuli of increasing brightness (cd/m^2). **E**) The graph shows the amplitude response (µV) to flicker stimuli of increasing frequencies (Hz). Mutant mice show a significant decrease of scotopic responses of photoreceptors (a-wave) at higher intensities (A) t-test, *: $p<0.05$

Figure 3. **Morphological alterations in *Sfrp1***$^{-/-}$ **retinas increase with age. A-D)** Semi-thin plastic frontal sections from 6 months-old wt and *Sfrp1*$^{-/-}$ retinas stained with toluidine blue. Black arrows in A,C indicate an organized column of photoreceptors, whereas white and red arrows indicate the outer and inner limit of the ONL. In B and D black and red arrows point to misplaced photoreceptor nuclei and discontinuous OLM respectively. **E-H)** Frontal cryostat sections from 6 months-old wt and *Sfrp1*$^{-/-}$ retinas immunostained with anti GNB3 (cones) or Rho (rods) antibodies and counterstained with Hoechst. White arrows in E,F point to the OS. Yellow and white arrows in H indicate accumulation of Rho in rod processes and cell bodies respectively. **I)** The graphs represent the thickness of the ONL in 12 months-old wt and *Sfrp1*$^{-/-}$ retinas showing a significant reduction in the mutants more evident in central regions. t-test; *: $p<0.05$, **: $p<0.01$, ***: $p<0.001$. Abbreviations. GCL: ganglion cell layer; INL: inner nuclear layer; on: optic nerve; ONL: outer nuclear layer.

Figure 4. **OLM is disrupted in the retina of *Sfrp1*$^{-/-}$ mice in association with an impoverishment of visual function. A-H)** TEM analysis of the retina from 6 months-old wt and *Sfrp1*$^{-/-}$ mice. Images show the OLM **(A,B)**, RPE **(C,D)** and photoreceptor-bipolar cells synapses **(E-H)**. White arrows in A and B indicate adherens junctions between Müller glial cell end-feet (red asterisks) and photoreceptors (black asterisks). White arrows in C,D point to melanosomes. Red and yellow arrows in G,H indicate synaptic terminal and mitochondria disorganization, respectively. **I-N)** The graphs show the ERG recordings of rods and rod bipolar cells (scotopic, I,J) and cones and cone bipolar cells (photopic, K,L) response to light of 9 months-old WT and *Sfrp1*$^{-/-}$ animals. **M,N)** The graphs represent the activity of photoreceptors (M) and cone photoreceptors (N) from 4 and 9 months-old Sfrp1 mice. Note that activity is expressed as a percentage of WT age-matched animals. Only 9 months-old Sfrp1 mice showed a significantly reduced activity relative to its control. t-test t-test; *: $p<0.05$, **: $p<0.01$. Abbreviations. bc: bipolar cell; hc: horizontal cell; r ribbon; sv: synaptic vesicles.

Figure 5. Proteolysis of OLM and OS proteins is increased in *Sfrp1*$^{-/-}$ retinas leading to an abnormal protein distribution. A-C) Western blot analysis of N-cadherin, PCDH21 and CRB1 content in total protein extracts from three weeks-old wt, *Sfrp1*$^{-/-}$ and *rd10* retinas, as indicated in the panels. For N-cadherin and PCDH21, membranes were probed with antibodies recognizing the respective C-terminal fragments (CTF). Graphs on the right of each panel indicate the rate of CTF proteolysis for N-cadherin **(A)** and PCDH21 **(B)**, calculated as CTF/FL, or the CRB1 levels **(C).** Plotted values are normalized to α-tubulin. **D-I**) Frontal cryostat sections from 6 months-old wt and *Sfrp1*$^{-/-}$ retinas immunostained with antibodies against N-cadherin, β-catenin, and GS as indicated in the panels. Sections are counterstained with Hoechst. White arrows in E, I indicate the gaps in the OLM. Scale bar calibration in I applies to all panels. Abbreviations: CTF: C-terminal fragment; FL: full length OLM: outer limiting membrane; ONL: outer nuclear layer.

Figure 6. *Sfrp1*$^{-/-}$ retinas are more prone to light-induced damage even in the presence of the *Rpe65*^{Leu450Met} protective variant. A-L) Frontal cryostat sections from 4 months-old control and *Sfrp1*$^{-/-}$ retinas carrying the *Rpe65*^{Leu450Leu} or the protective *Rpe65e*^{Leu450Met} variants before and after light induced-damage, as indicated in the panels. Sections were immunostained with antibodies against Rho (rods, red) or GNB3 (cones, green) and

counterstained with Hoechst. **M, N)** The graphs represent the ONL thickness (measures were taken in cryostat frontal sections of the eye at the level of the optic disk). in the different conditions. Scale bar in L applies to all panels. Abbreviations: ONL: outer nuclear layer; OPL: outer plexiform layer; OS outer segment.

Figure 7. Loss of reduces the ERG response after light-induced damage even in the *Rpe65*^{Leu450Leu} variant. A-D) The graphs show the a- and b-wave amplitude (µV) of the scotopic (rods and rod bipolar cells, A, B) and photopic (cones and cone bipolar cells, C, D) ERG response from 4 months-old WT and *Sfrp1*$^{-/-}$ animals to flash light stimuli of increasing brightness (cd/m2). **E**) The graph shows the amplitude response (µV) to flicker stimuli of increasing frequencies (Hz). ANOVA with post hoc Tukey. * indicates significant differences between Sfrp1 untreated and light-damage mice. # indicates significant differences between Sfrp1 and WT animals subjected to light damage. * or #: $p<0.05$.

Figure 8.

Proposed model for the defects observed in the *Sfrp1*$^{-/-}$ mice. See the discussion for details. Abbreviations: IN: inner segment; OLM: outer limiting membrane; OS: outer segment.

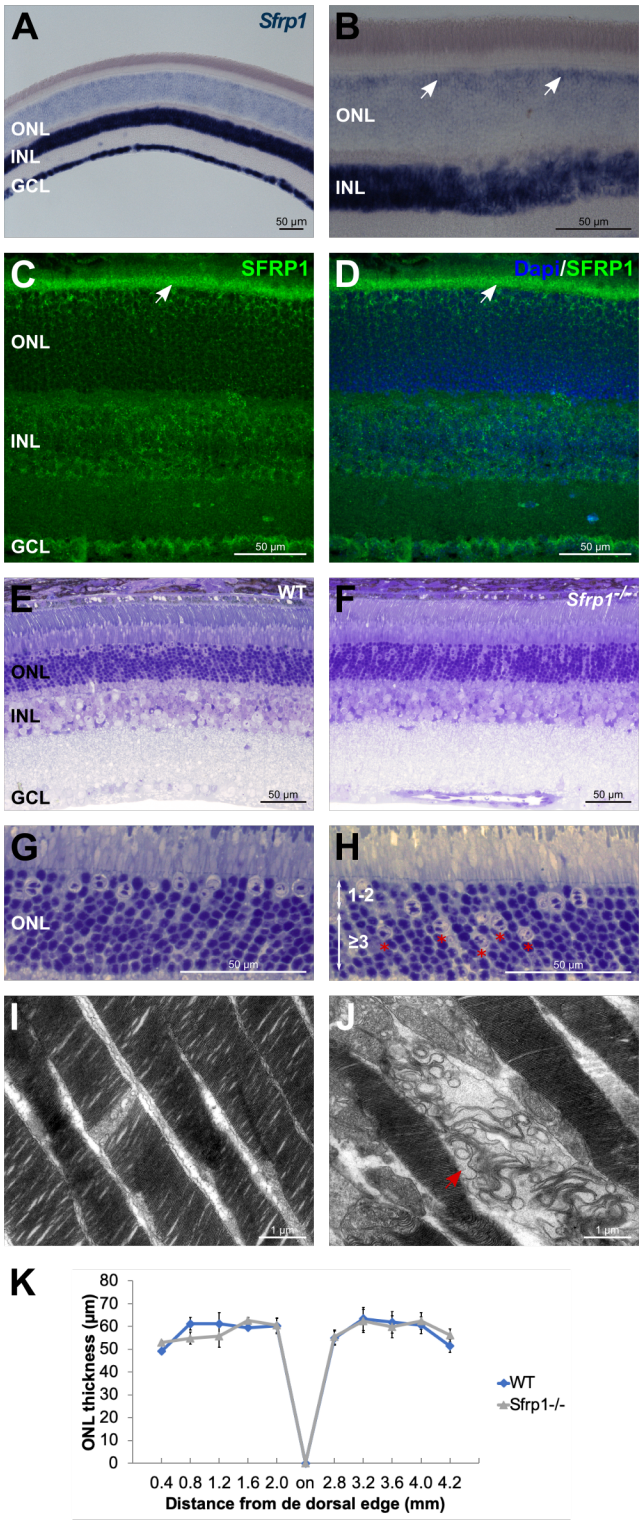

Figure 1

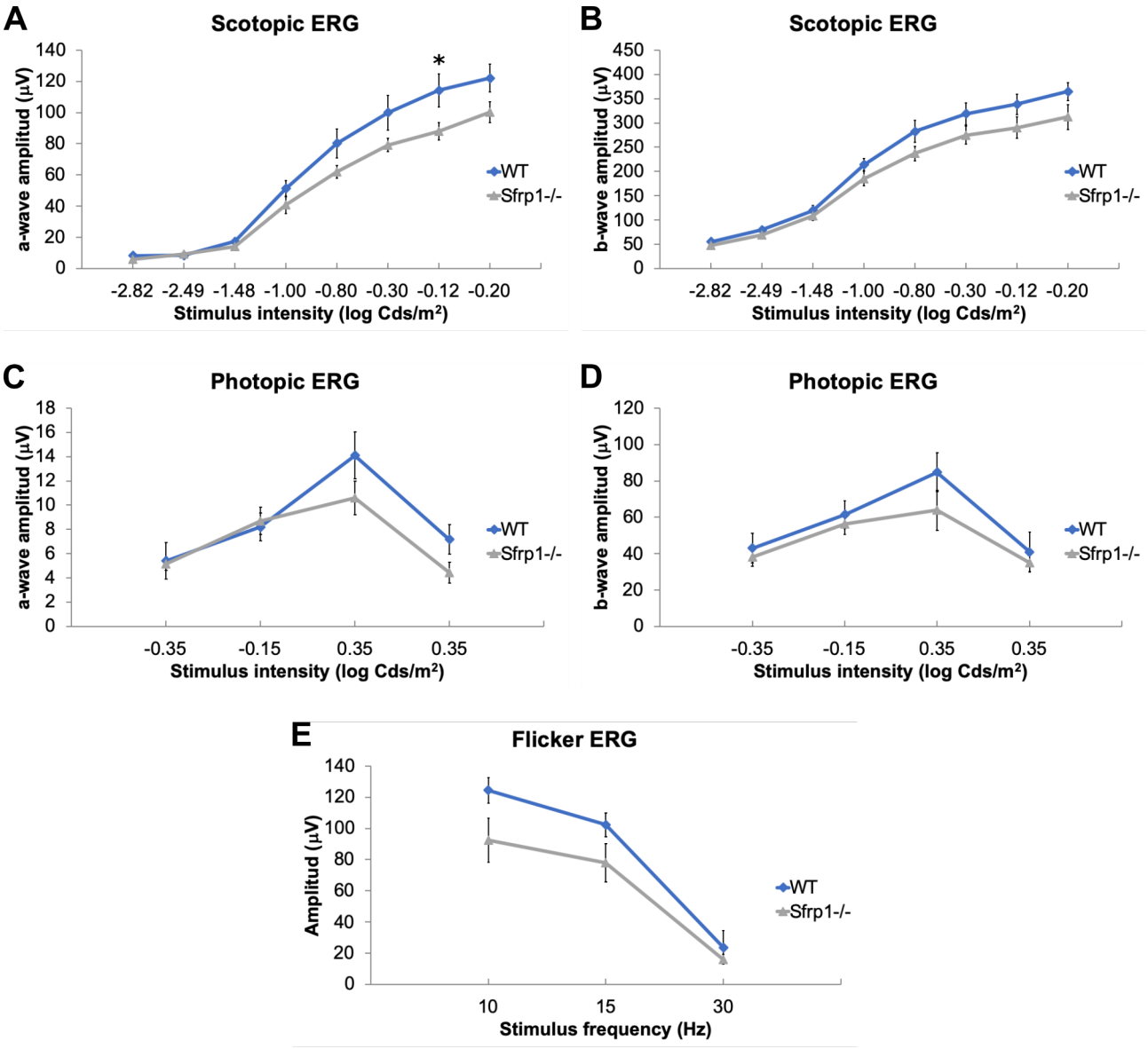

Figure 2

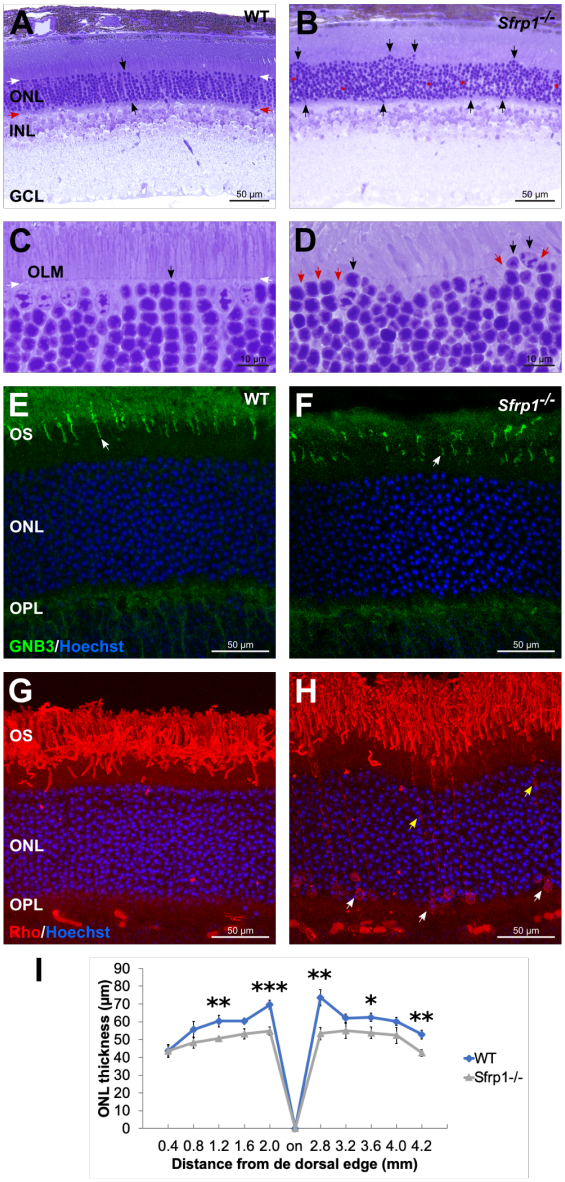

Figure 3

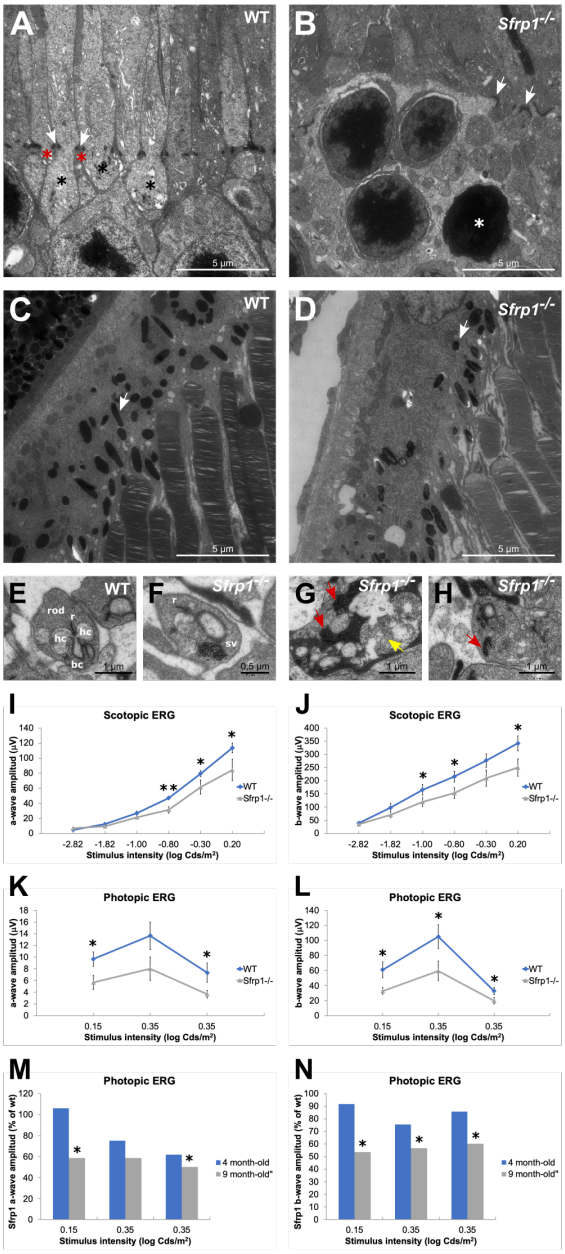

Figure 4

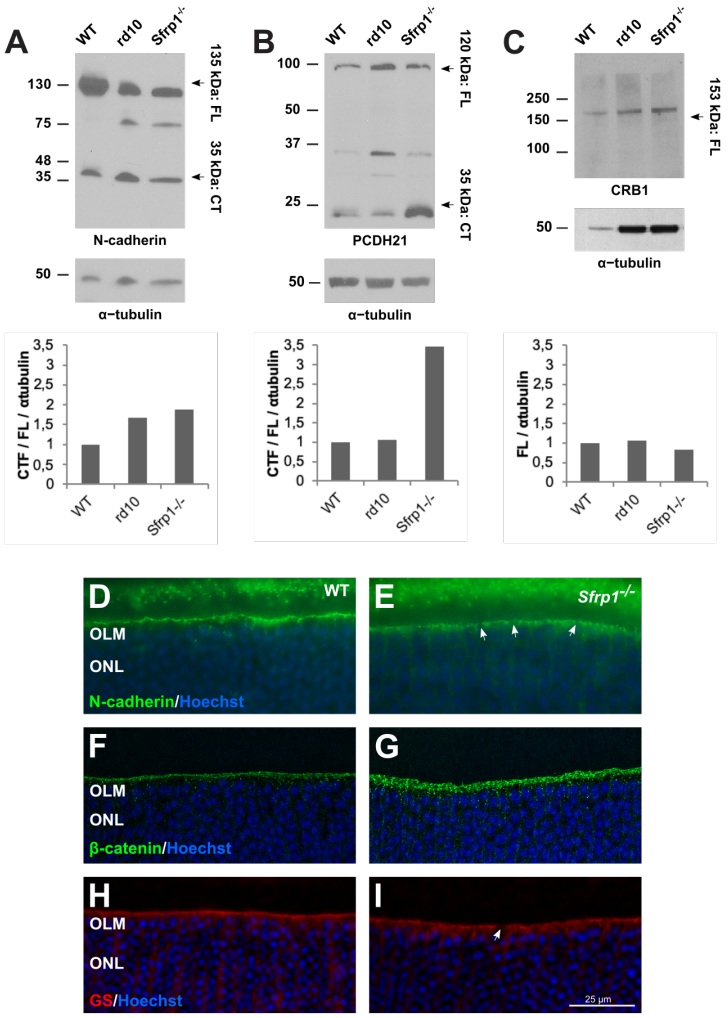

Figure 5

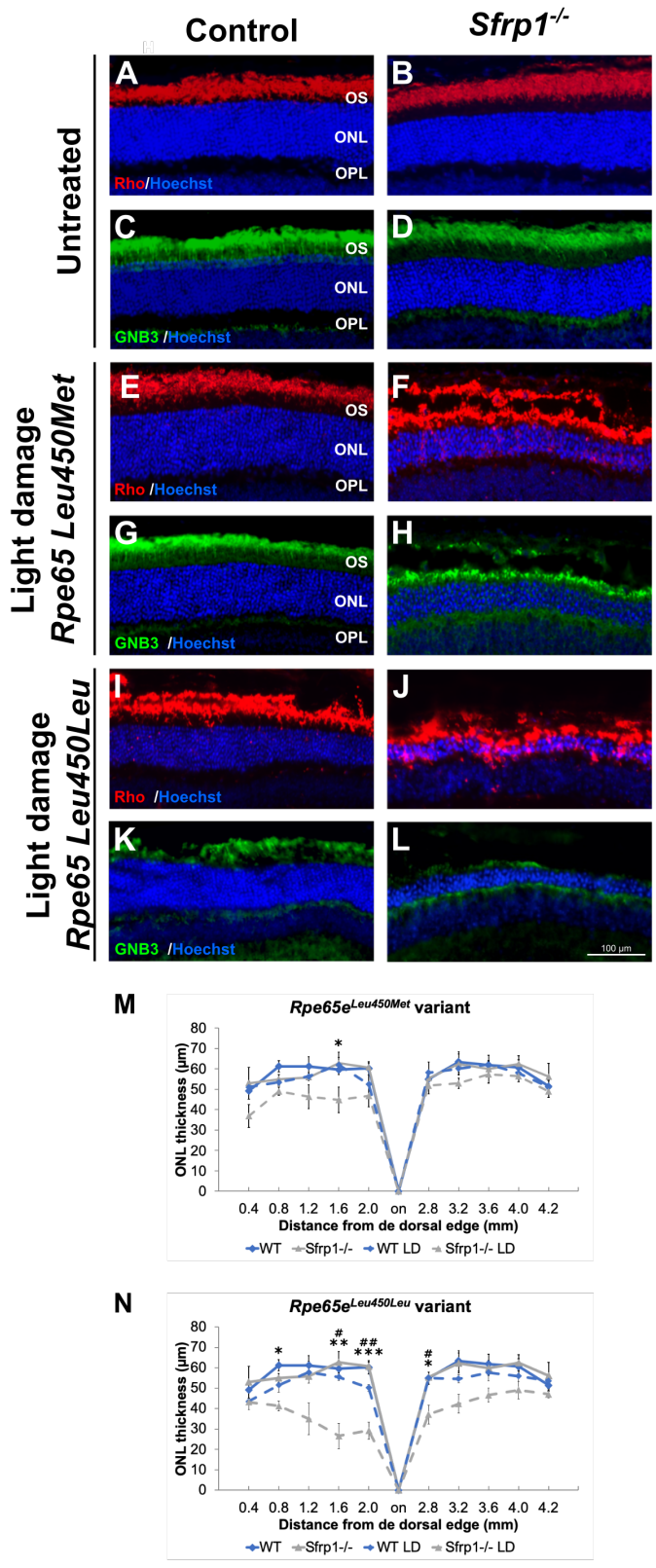

Figure 6

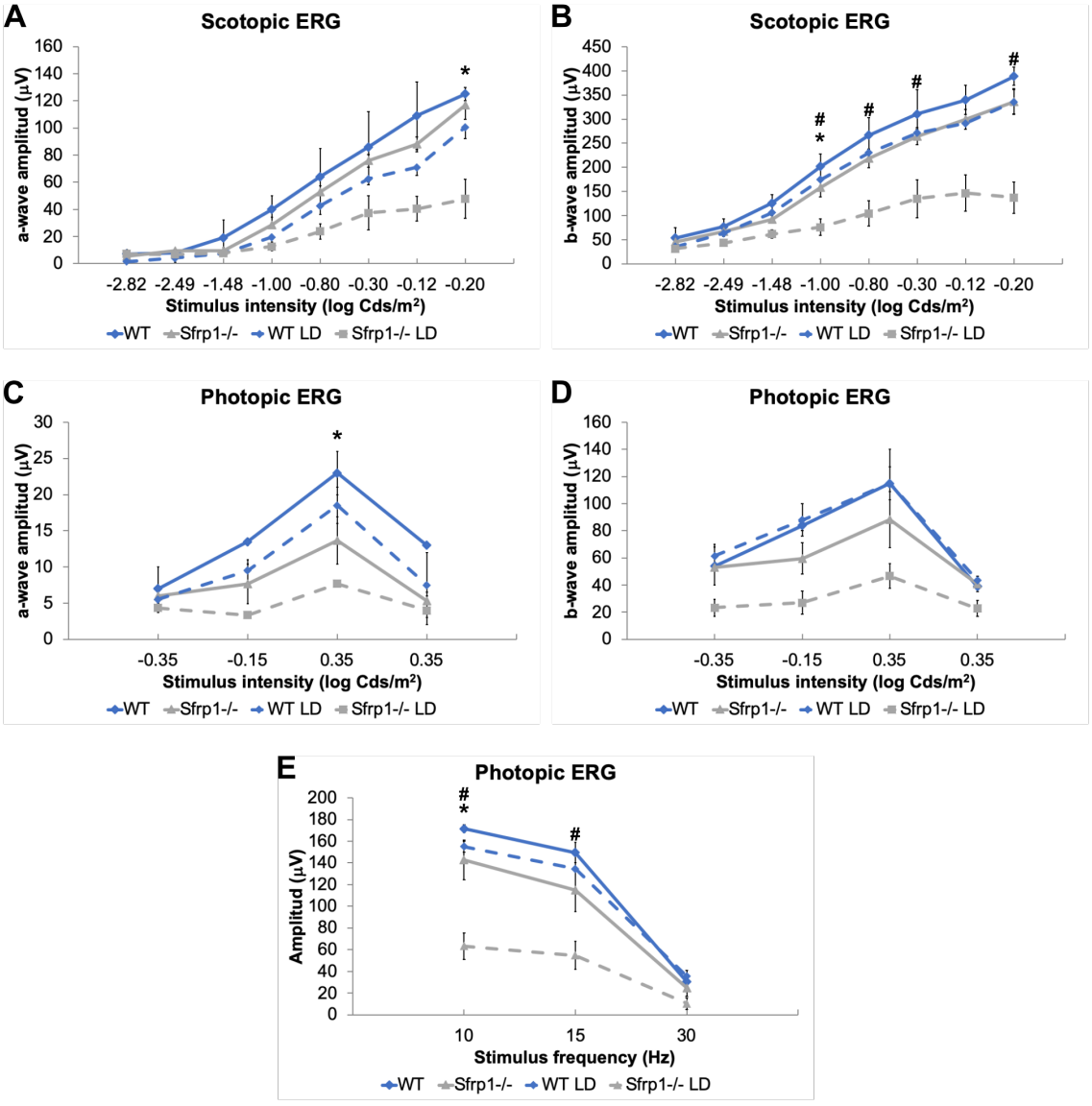

Figure 7

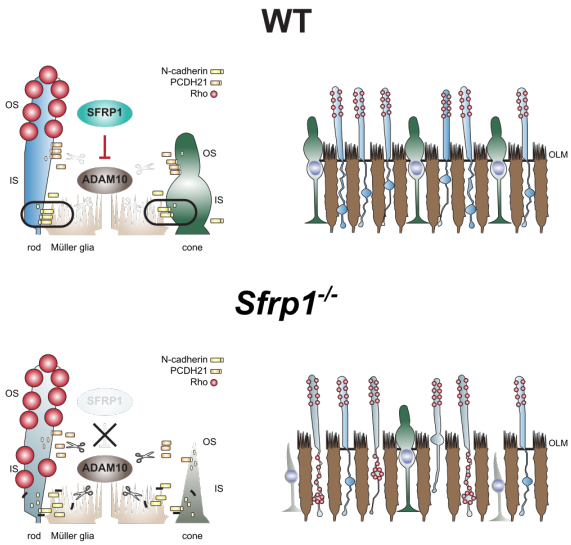

Figure 8